# Fluorescence lifetime imaging microscopy for brain tumor image-guided surgery

**Yinghua Sun**
University of California
Davis, Department of Biomedical Engineering
Davis, California 95616
and
National Science Foundation
Center for Biophotonics Science & Technology
Sacramento, California 95817

**Nisa Hatami**
**Matthew Yee**
**Jennifer Phipps**
University of California
Davis, Department of Biomedical Engineering
Davis, California 95616

**Daniel S. Elson**
Imperial College London
Institute of Biomedical Engineering
London SW7 2AZ, United Kingdom

**Fredric Gorin**
University of California
Davis, Department of Neurology
Davis, California 95616

**Rudolph J. Schrot**
University of California
Davis, Department of Neurological Surgery
Sacramento, California 95817

**Laura Marcu**
University of California
Davis, Department of Biomedical Engineering
Davis, California 95616
and
National Science Foundation
Center for Biophotonics Science & Technology
Sacramento, California 95817

**Abstract.** We demonstrate for the first time the application of an endoscopic fluorescence lifetime imaging microscopy (FLIM) system to the intraoperative diagnosis of glioblastoma multiforme (GBM). The clinically compatible FLIM prototype integrates a gated (down to 0.2 ns) intensifier imaging system with a fiber-bundle (fiber image guide of 0.5 mm diameter, 10,000 fibers with a gradient index lens objective 0.5 NA, and 4 mm field of view) to provide intraoperative access to the surgical field. Experiments conducted in three patients undergoing craniotomy for tumor resection demonstrate that FLIM-derived parameters allow for delineation of tumor from normal cortex. For example, at 460±25-nm wavelength band emission corresponding to NADH/NADPH fluorescence, GBM exhibited a weaker florescence intensity (35% less, $p$-value $<0.05$) and a longer lifetime $\tau_{\text{GBM-Amean}}=1.59\pm0.24$ ns than normal cortex $\tau_{\text{NC-Amean}}=1.28\pm0.04$ ns ($p$-value $<0.005$). Current results demonstrate the potential use of FLIM as a tool for image-guided surgery of brain tumors. 
[DOI: 10.1117/1.3486612]

Keywords: fluorescence lifetime imaging microscopy; tissue autofluorescence; endoscopy; malignant glioma; brain tumors; intraoperative cancer diagnosis.

Paper 10290LRR received Jun. 7, 2010; revised manuscript received Aug. 10, 2010; accepted for publication Aug. 12, 2010; published online Oct. 7, 2010.

## 1 Introduction

Glioblastoma multiforme (GBM) is the most common and aggressive brain tumor in humans, accounting for 52% of all brain tumor cases.[1,2] The median survival is 12 to 15 months. Optimal therapy consists of maximal safe surgical resection, followed by adjuvant chemoradiotherapy.[3] Several studies demonstrate that the extent of surgical resection is a determinant of progression-free and overall survival.[2] Achieving a gross total resection is surgically challenging, because the normal and tumor-bearing brain can be similar in intraoperative appearance.[3] A conservative resection by the surgeon can lead to suboptimal tumor debulking, whereas an aggressive technique may encroach on functionally significant brain. Various techniques have been employed to aid the neurosurgeon during tumor resection, including intraoperative MRI, neuronavigation, functional mapping via cortical stimulation, and ultrasonography.[3] None of these techniques allows the direct pathologic discrimination of tissue.[3]

The ability to rapidly distinguish tumor from nontumor would provide a powerful tool to augment neurosurgical judgment during tumor resection. Recent work has demonstrated the potential of laser-induced fluorescence spectroscopy

Address all correspondence to: Laura Marcu, Ph.D., University of California, Davis, Department of Biomedical Engineering, 451 Health Science Drive, GBSF, Davis, CA 95616 Tel: 530-732-0288; E-mail: lmarcu@ucdavis.edu

1083-3668/2010/15(5)/056022/5/$25.00 © 2010 SPIE

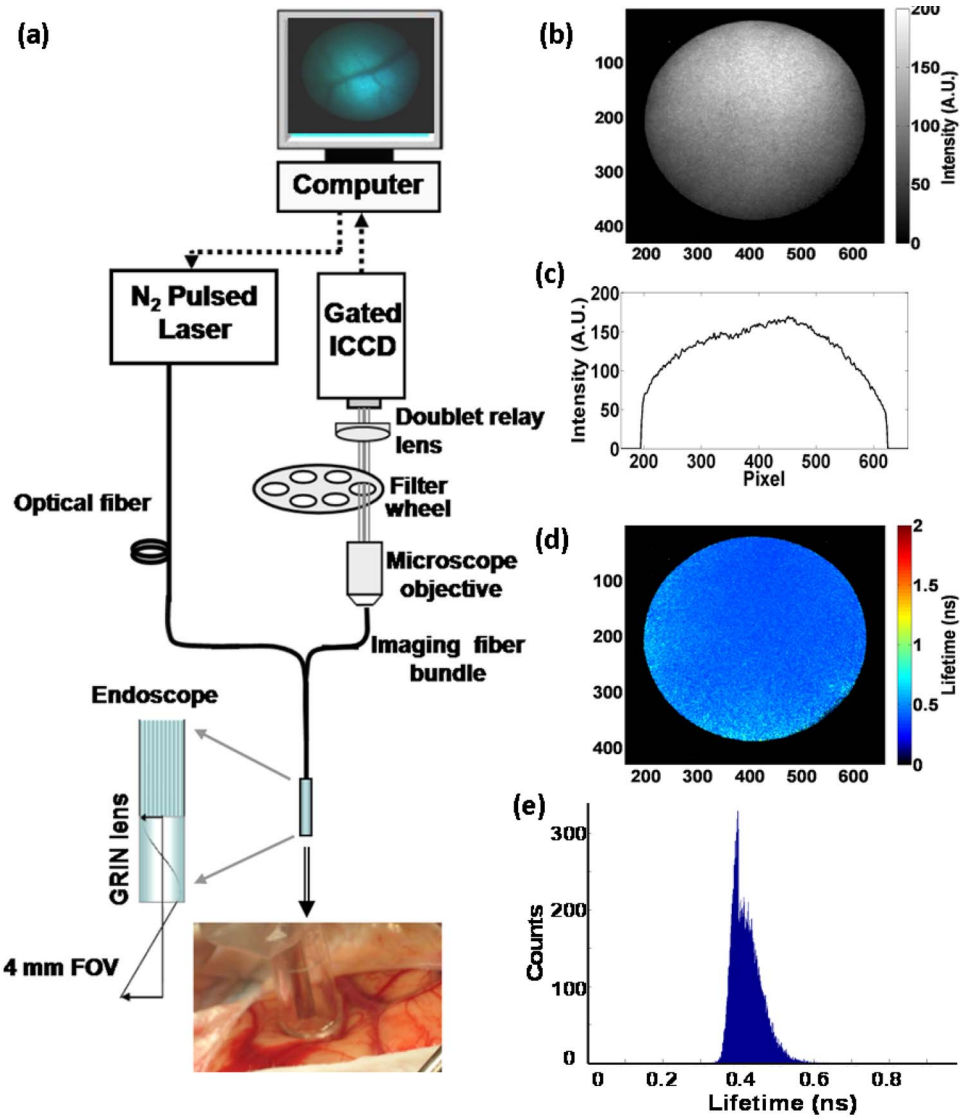


**Fig. 1** (a) Schematic of the FLIM instrument setup, including a picture of the tip of the imaging bundle probe positioned on the interrogated area of the cortex. (b) Fluorescence intensity image of rhodamine B and (c) a cross section of the intensity distribution (profile). Note that The fluorescence intensity is higher in the center of the image when compared to the edge of the image. (d) Fluorescence average lifetime image and (e) fluorescence average lifetime histogram of the rhodamine B solution measured and analyzed with the FLIM system. The pixel coordinates are shown on the left and bottom side of the images in (b) and (d).

(LIFS)[4–7] and time-resolved LIFS (TR-LIFS)[6–8] of endogenous fluorophores as a diagnostic tool in brain tumor operations.

The goal of this pilot study is to test a prototype endoscopic fluorescence lifetime imaging microscopy (FLIM) device for intraoperative evaluation and potential diagnosis of brain tumors. We evaluate whether the fluorescence lifetime contrast can be achieved between normal brain and brain tumor (glioblastoma) areas as identified diagnostic methods typically used during neurosurgical procedures (e.g., gross pathology and preoperative MRI images) and neurosurgeon experience. FLIM is particularly appropriate for intraoperative application, because the time-resolved images are minimally affected by factors that often confound point spectroscopic analysis, including irregular tissue surfaces, nonuniform illumination, and endogenous absorbers such as blood in the operative field.[9]

## 2 Materials and Methods

*Instrumentation.* The FLIM apparatus (Fig. 1) consisted of a gated intensified charge-coupled device (ICCD) camera, a pulsed laser, a flexible fiber-image guide-based endoscope, and a filter wheel. This system was adapted from our previously reported FLIM apparatus.[9] Modifications were made for intraoperative use, including portability, remote fiber optic access to patients, fiber-probe sterilization, and medical safety. Figure 1(a) is a schematic of the instrument. The positioning of the fiber probe on the brain is also depicted. Briefly, tissue autofluorescence was induced by a pulsed nitrogen laser

(337 nm, 700 ps, MNL 205 nitrogen, LTB Lasertechnik, Berlin). A customized semiflexible endoscope probe (3 m long) remotely delivered the excitation laser, and the fluorescence emission was imaged using a gradient index (GRIN) lens (NA=0.5, 0.5 mm diam, and 4-mm field of view) cemented to a fiber image guide (0.6 mm diameter, 10,000 fibers). The fluorescence emitted from the proximal end of the fiber bundle was projected onto the fast-gated ICCD (4 Picos, Stanford Computer Optics, Berkeley, California). A bandpass filter with a center wavelength of 460 nm and a bandwidth of 50 nm was used. Data acquisition time for each measurement was ~2 min, including one steady-state image and a series of up to 29 time-gated images (0.5-ns gating time and 0.5-ns relative delay-time interval). During imaging, the probe was gently positioned perpendicular to the tissue surface and held with a Greenberg device to minimize the moving artifacts.

*Sample illumination through endoscope probe.* The energy density delivered at the tissue surface was 0.16 $mJ/cm^2$ per pulse (20 times lower than the maximum permissible exposure value of 3.2 $mJ/cm^2$ for UV lasers according to the American National Standard for Safe Use of Lasers). Figures 1(b) and 1(c) demonstrate the illumination intensity at a plane located 4 mm in front of the endoscope probe for a solution of rhodamine B (0.1 mM in methanol). The fluorescence intensity is strong in the center but drops significantly at the edge. This is due to the current endoscope that did not permit uniform illumination of the sample. Vignetting also occurs at the edge of the field. Despite this, the mean average fluorescence lifetime ($0.44 \pm 0.03$ ns) is uniform across the entire surface [Figs. 1(d) and 1(e)] after numerical deconvolution of lifetime values, as described next.

*Image processing.* Images were analyzed using the Laguerre polynomial deconvolution technique to calculate the fluorescence impulse response function, average fluorescence lifetime ($\tau_f$), integrated intensity, and Laguerre coefficients (LECs).[10] The Laguerre functions contain a built-in exponential term that results in a convenient expansion of exponential decays while also forming a complete orthogonal set that allows fast and complete expansion. The first four Laguerre functions were sufficient to recreate the fluorescence decay. The resulting function can then be used to calculate $\tau_f$ (by computing the interpolated time at which the intensity falls to 1/e of the initial intensity) and integrated intensity of the data. This technique[10] enables fast lifetime processing. Tissue FLIM images ($480 \times 736$ pixels) presented took less than 60 s to process on a PC with an Intel Core 2 CPU 6600 at 2.40 GHz and 1-GB RAM running Matlab.

*Statistical analysis.* To distinguish between tissue types (tumor versus normal), FLIM data represented by multiple parameters (fluorescence intensity, $\tau_f$, and LECs values) were evaluated using one-way analysis of variances (ANOVA). A $p$-value $<0.05$ was used as criteria for achieving statistical significance.

*Validation on human subjects.* FLIM experiments were conducted on three patients undergoing craniotomy and resection of glioblastoma. 13 sites were examined, four from normal cortex (NC), seven from GBM-infiltrated cortex (GBM), and two from brain-tumor interface (BTI). Areas were identified by the neurosurgeon based on an intraoperative MRI-guided neuronavigation system and by visual inspection of the operative site. The study was approved by the University of California Davis Institutional Review Board. The FLIM instrument (on a mobile cart) was brought to the operating room and the distal end of the endoscopic probe was placed in a sterilized protective tube that extended 4 mm beyond the end of the probe. For intraoperative measurement, the protective sterile tube was positioned perpendicular to the tissue surface, gently resting on the brain. Tissue biopsies were taken from tumor areas for histopathologic correlation.

## 3 Results and Discussion

Figure 2 depicts representative images for fluorescence intensity and $\tau_f$ in NC, GBM, and BTI. The mean $\pm$ standard deviation values of $\tau_f$ for one representative area are defined as individual-mean average fluorescence lifetime ($\tau_{\text{Imean}}$). Table 1 shows the mean $\pm$ standard deviation values of each FLIM-derived parameter of all measurements from 13 sites in all three patients, where nine sites are from GBM (three areas from each patient) and four sites are normal (two areas from patient 1 and one area from patients 2 and 3). The mean $\pm$ standard deviation values of $\tau_f$ for all patients grouped by tissue type is given as $\tau_{\text{Amean}}$.

*Fluorescence intensity image.* In NC, a clear network of blood vessels was observed in the intensity image [Fig. 2(a)] most likely caused by the strong absorption of hemoglobin.[11] The center region of the intensity image was bright due to the uneven illumination of the endoscopic probe. Similar features were observed for intensity images of GBM [Fig. 2(b)] and BTI [Fig. 2(c)] sites. Overall, the fluorescence intensity was higher for areas identified as NC compared to GBM (Table 1). These findings are in agreement with earlier LIFS studies,[4,5,11,12] which demonstrated that fluorescence intensity in GBM was lower compared with NC between 450 and 480 nm. It is well documented[4,5] that upon UV excitation, the main brain tissue fluorophores emitting at these wavelengths are the reduced nicotinamide adenine dinucleotides NADH and reduced nicotinamide adenine phosphate dinucleotides NADPH in both free and protein-bound form. The concentration of the NADH is approximately five times greater than that of the NADPH.[13] Changes in autofluorescence in this spectral band were attributed to an alteration of the contribution of these dinucleotides to the overall emission, and to changes of the total amount of redox equilibrium and the free/bound condition of these coenzymes.[4,13]

*Fluorescence lifetime image.* NC showed relatively uniform $\tau_f$ values across the entire area [Fig. 2(d)], as demonstrated by a narrow $\tau_f$ histogram [Fig. 2(g)] with a value of $\tau_{\text{NC-Imean}} = 1.23 \pm 0.09$ ns. Neither the nonuniform illumination at the tissue surface nor the presence of blood affected the $\tau_f$ values. This emphasizes the more robust nature of time-resolved measurement versus intensity measurements when implemented *in vivo*, where uniform illumination can be difficult to achieve due to tissue irregularities as well as the presence of blood in the surgical field. For a few measurements of NC, we noticed a slight increase in $\tau_f$ to ~1.5 ns in areas containing blood

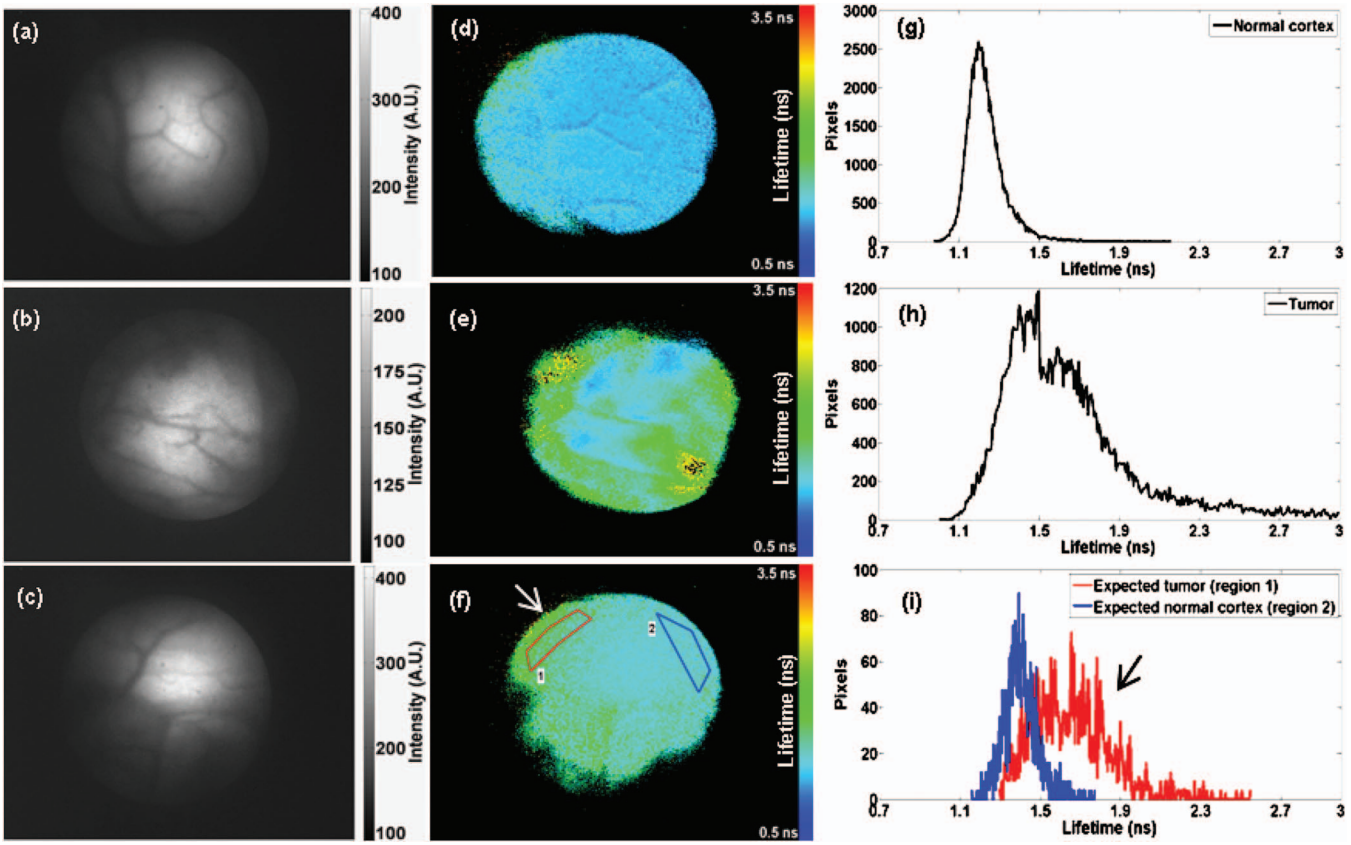


**Fig. 2** Representative fluorescence intensity and lifetime images. (a), (b), and (c) are intensity images. (d), (e), and (f) are fluorescence average lifetime images. (g), (h), and (i) show fluorescence lifetime histograms. (i) depicts lifetime histograms of two ROIs identified in (f), where the arrow indicates the tumor area. For each image, the average lifetime value was retrieved from the $2\times2$ binning pixel of four original pixels ($2\times2$ square). All average lifetime values for each binning pixel in the ROI were plotted together to show a histogram of average lifetime distribution.

vessels. While the exact origin of this trend is not known, this trend is clearly related to the presence of the blood vessel, as observed in the fluorescence intensity image and by the eye. Possible explanations include the contribution to the fluorescence from structural protein in the blood vessel, or the decrease of oxygen concentration in these regions, which in turn increases the relative concentration of bound NADH, or the selective absorption of the fluorescence by the blood.

GBM sites exhibited nonuniform distribution of $\tau_f$ values across the interrogated area. The lifetime histogram [Fig. 2(h)] depicts a higher $\tau_f$ with a broad distribution ($\tau_{\text{GBM-Imean}}=1.64\pm0.33$ ns) compared with NC. A few subareas exhibited shorter $\tau_f$ values comparable with that of normal cortex. We ascribe this to the variable depth at which the tumor is infiltrated within the cortex with respect to the surface of the cortex. While the entire area is identified as tumor, in some subareas the tumor can be below the penetration depth ($\sim$200 to 300 $\mu$m) of the excitation wavelength, thus fluorescence was mainly collected from normal tissue on top of the tumor. The BTI sites also exhibited a nonuniform distribution of the fluorescence lifetime values. However, the $\tau_f$ values were segregated, with longer values ($\tau_{\text{Imean}}=1.66\pm0.20$ ns) in tumor versus normal cortex ($\tau_{\text{Imean}}$

**Table 1** Summary of intensity ($I_{\text{Amean}}$), average lifetime ($\tau_{\text{Amean}}$), and Laguerre coefficients ($\text{LEC}_{\text{Amean}}$). Change percentage (and corresponding *p*-value) is for the relative change of the GBM versus NC values.

| | Intensity (au) | $\tau_f$ (ns) | LEC-0 (au) | LEC-1 (au) | LEC-2 (au) | LEC-3 (au) |
|---|---|---|---|---|---|---|
| NC ($n=4$) | 1091±253 | 1.28±0.04 | 0.21±0.03 | 0.26±0.02 | 0.24±0.02 | 0.27±0.01 |
| GBM ($n=9$) | 704±248 | 1.59±0.24 | 0.39±0.15 | 0.21±0.03 | 0.12±0.11 | 0.21±0.05 |
| Change% | −35 | 24 | 87.55 | −16.98 | −46.95 | −23.56 |
| *p*-value | 0.0199 | 0.0027 | 0.0160 | 0.0045 | 0.0372 | 0.0037 |

$=1.40\pm0.09$ ns) [Fig. 2(i)]. Parameters derived from FLIM data (both $\tau_f$ and LECs) demonstrated significant differences between GBM and NC. Overall, we determine faster decay dynamics for NC compared to GBM. We note also that LEC-0, which is associated with the fast decay component of the fluorescence decay curve,[10] presents the largest relative change ($>80\%$) with a lower value in NC versus GBM.

The $\tau_f$ of NADH and NADPH depends on their bound-free forms, with a range from subnanosecond values in the free form to a few nanoseconds in the protein-bound form.[14,15] The $\tau_f$ of brain tissues in this study ranged between 1.2 to 2.6 ns, most likely reflecting changes in the bound-free NADH/NADPH equilibrium between normal and tumor conditions. These values suggest that fluorescence emission of brain tissue is dominated by the protein-bound form of these coenzymes, with a relatively higher contribution of the bound form to the GBM fluorescence when compared to that of NC. The fluorescence lifetime of NADH and NADPH in brain tissues *in vivo* has been underinvestigated. Vishwasrao et al.[13] reported NADH kinetics in brain hippocampus slices in normoxic and hypoxic conditions, where the latter showed a shorter $\tau_f$ than the former. In our previous TR-LIFS studies,[6] we also observed similar or slightly longer $\tau_f$ at 460 nm for GBM compared with normal cortex, a trend that is in agreement with the current study. Due to different experimental conditions, no extensive comparison with other studies can be made, however our current findings demonstrate that imaging lifetimes allow normal versus tumor to be distinguished

The main challenge in the validation of FLIM results is the ability to conduct conventional histopathological analysis of all interrogated areas, so that optical results can be correlated to local pathologies. This is a significant challenge for brain tissue diagnosis, where biopsy is limited to areas of tumor involvement. Neurosurgical techniques for GBM resection do not typically involve obtaining pathologically tumor-free tissue margins, as is the case for cancers operated on in other regions of the body. Instead, GBM resection is limited to the areas of gross tumor involvement, or in the case of malignant GBMs, to the enhancing and necrotic portions. Thus, in the current study the validation of the FLIM results was mainly based on gross pathology, MRI data, and neurosurgeon experience. Another limitation is the sampling error that results from the heterogeneous tissue composition of the tumor, which can contain heterotopic areas of hypervascularity, necrosis, ischemia, and degrees of malignant degeneration.

## 4 Conclusion

This study demonstrates for the first time the feasibility of a fiber image guide (endoscopic) FLIM system in a neurosurgical setting for intraoperative observation and characterization of brain tissue autofluorescence. Analysis of FLIM data recorded in patients undergoing craniotomy and resection of GBM demonstrate that fluorescence lifetime contrast can be achieved between tumor sites and normal cortex. A more extensive study in a larger number of patients and new strategies that allow for the validation of optical measurements against conventional histopathology are required to fully characterize the ability of FLIM to delineate tumor margins intraoperatively. However, these results demonstrate that fluorescence lifetime contrast between tumor and normal cortex can be consistently achieved and is independent of tissue illumination, irregular brain tissue surface, and presence of blood in the surgical field.

### Acknowledgments

This study was supported in part by the University of California Davis Cancer Center and NIH Grant HL067377, RO1 NS40489 and R01 NS060880.

### References

1. A. Brandes, A. Tosoni, E. Franceschi, M. Reni, G. Gatta, and C. Vecht, "Glioblastoma in adults," *Crit. Rev. Oncol. Hematol.* **67**, 139–152 (2008).
2. N. Sanai and M. S. Berger, "Glioma extent of resection and its impact on patient outcome," *Neurosurgery* **62**, 753–764 (2008).
3. H. I. Robins, A. B. Lassman, and D. Khuntia, "Therapeutic advances in malignant glioma: current status and future prospects," *Neuroimaging Clin. N. Am.* **19**, 647–656 (2009).
4. A. C. Croce, S. Fiorani, D. Locatelli, R. Nano, M. Ceroni, F. Tancioni, E. Giombelli, E. Benericetti, and G. Bottiroli, "Diagnostic potential of autofluorescence for an assisted intraoperative delineation of glioblastoma resection margins," *Photochem. Photobiol.* **77**, 309–318 (2003).
5. W. C. Lin, A. Mahadevan-Jansen, M. D. Johnson, R. J. Weil, and S. A. Toms, "In vivo optical spectroscopy detects radiation damage in brain tissue," *Neurosurgery* **57**, 518–525 (2005).
6. P. V. Butte, Q. Fang, J. A. Jo, W. H. Yong, B. K. Pikul, K. L. Black, and L. Marcu, "Intra-operative delineation of primary brain tumors using time-resolved fluorescence spectroscopy," *J. Biomed. Opt.* **15**, 027008 (2010).
7. Y. G. Chung, J. A. Schwartz, C. M. Gardner, R. E. Sawaya, and S. L. Jacques, "Diagnostic potential of laser-induced autofluorescence emission in brain tissue," *J. Korean Med. Sci.* **12**, 135–142 (1997).
8. L. Marcu, J. A. Jo, P. V. Butte, W. H. Yong, B. K. Pikul, K. L. Black, and R. C. Thompson, "Fluorescence lifetime spectroscopy of glioblastoma multiforme," *Photochem. Photobiol.* **80**, 98–103 (2004).
9. Y. Sun, J. Phipps, D. S. Elson, H. Stoy, S. Tinling, J. Meier, B. Poirier, F. S. Chuang, D. G. Farwell, and L. Marcu, "Fluorescence lifetime imaging microscopy: in vivo application to diagnosis of oral carcinoma," *Opt. Lett.* **34**, 2081–2083 (2009).
10. J. A. Jo, Q. Fang, T. Papaioannou, and L. Marcu, "Fast model-free deconvolution of fluorescence decay for analysis of biological systems," *J. Biomed. Opt.* **9**(4), 743–752 (2004).
11. W. C. Lin, S. A. Toms, M. Johnson, E. D. Jansen, and A. Mahadevan-Jansen, "In vivo brain tumor demarcation using optical spectroscopy," *Photochem. Photobiol.* **73**, 396–402 (2001).
12. G. Bottiroli, A. C. Croce, D. Locatelli, R. Nano, E. Giombelli, A. Messina, and E. Benericetti, "Brain tissue autofluorescence: an aid for intraoperative delineation of tumor resection margins," *Cancer Detect. Prev.* **22**, 330–339 (1998).
13. H. D. Vishwasrao, A. A. Heikal, K. A. Kasischke, and W. W. Webb, "Conformational dependence of intracellular NADH on metabolic state revealed by associated fluorescence anisotropy," *J. Biol. Chem.* **280**, 25119–25126 (2005).
14. J. R. Lakowicz, *Principles of Fluorescence Spectroscopy*, 2nd ed., Kluwer Academic/Plenum, New York (1983).
15. R. Niesner, P. Narang, H. Spiecker, V. Andresen, K. H. Gericke, and M. Gunzer, "Selective detection of NADPH oxidase in polymorphonuclear cells by means of NAD(P)H-based fluorescence lifetime imaging," *J. Biophys.* **2008**, 602639 (2008).